PROCEEDINGS OF SCIENCE

Top quark properties measurements with the ATLAS detector

Francesco Spanò, on behalf of the ATLAS collaboration*
Royal Holloway, University of London
E-mail: francesco.spano@cern.ch

Precise measurements of the properties of the top quark test the Standard Model (SM) and can be used to constrain new physics models. The dataset collected by ATLAS in LHC pp collisions at $\sqrt{s}$ = 8 TeV is used to perform a variety of such measurements. In the SM the top quark is predicted to decay almost exclusively into a W boson and a b-quark. Measurements of the W-helicity and spin correlations in $t\bar{t}$ production are presented as well as new measurements of CP asymmetries in b-hadron decays using top-quark events. As it may be significantly enhanced by the presence of new physics, the $t\bar{t}$ production charge asymmetry is measured inclusively and differentially in the lepton+jets and dilepton channels, including a dedicated measurement for highly boosted top quarks. The first direct ATLAS measurement of the top-quark width is presented.

EPS-HEP 2017, European Physical Society conference on High Energy Physics
5-12 July 2017
Venice, Italy

*Speaker.

PoS(EPS-HEP2017)469

1 Introduction

The top quark is the most massive known fundamental fermion described by quantum field theory, the only one with a mass of the same order magnitude of the electroweak symmetry scale [1]. Being embedded in the standard model (SM) interaction scheme, it is characterized by additional properties (quantum numbers) beyond its mass and spin: the charges associated to electromagnetic, strong and weak interactions. It is the weak interaction, with its identity changing decays, that is mostly responsible for the size of the top-quark width. Due to the combination of its large mass and the weak coupling, the lifetime of the top quark is so much smaller than its spin decorrelation time that the top-quark decays before its spin flips i.e. spin information is passed to decay products undiluted by hadronisation effects [2, 3] allowing direct observation of such properties at the decay level. In addition, due to the conservation of chirality in gauge interactions, the like/unlike helicity configuration of incoming parton pairs in strong interactions in pp collisions results into producing top-quark pairs for which the spin of the top and antitop are correlated [4, 5]. As the spins of top-quark decay products are also correlated with the spin of the top quark and spin information is mantained beyond hadronisation in top-quark decay, the angles of the $t\bar{t}$ decay products are expected to be correlated [4]. Additional correlations result from angular asymmetries due to NLO interference effects in $t\bar{t}$ production [6] and from CP violation in b-quark decays from $t\bar{t}$ pairs [7].

Within this theoretical framework, the SM predicts resulting observable consequences in $t\bar{t}$ production and decay at hadron colliders: the values of the fractions of $t\bar{t}$ events produced in a given W boson polarisation state (helicity fractions) in the t $\rightarrow W\ b$ decay, no polarization for the top quark and non-zero correlation between the spins of the top and antitop quark in $t\bar{t}$ production. The SM also predicts the entire structure of the spin density matrix [8] for $t\bar{t}$ production and decay, it foresees that the top- and antitop-quark angular distributions are different due to NLO interference effects and that the values of CP violation asymmetries are smaller than 10^{-3} in $t\bar{t}$ events.

This review illustrates measurements of angular and asymmetry properties in top-quark production and decay, using data collected by the ATLAS detector [9] in pp collisions produced by the Large Hadron Collider (LHC) at a center of mass energy ($\sqrt{s}$) of 8 TeV. The data set corresponds to an integrated luminosity of up to 20.3 fb^{-1}. Such measurements test the SM predictions resulting from the interplay of top-quark spin and charges, they can be sensitive to presence of new physics phenomena which foresee deviations from the features predicted by the SM and they complement the ATLAS measurements of the top-quark mass [10] and of its production rates [11].

2 The Wtb vertex in top-quark decay: W polarisation

The measurement of the polarisation of the W boson [12] is sensitive to the V - A structure of the Wtb vertex and it tests the presence of additional couplings beyond those compatible with the SM symmetries. The polarisation value is obtained by measuring the cosine of θ^*, the angle between the direction of the d-type W boson decay product (lepton, d-, s-quarks) and the reversed direction of the b-quark from the top-quark decay, all considered in the W boson rest frame. The W boson decay products are

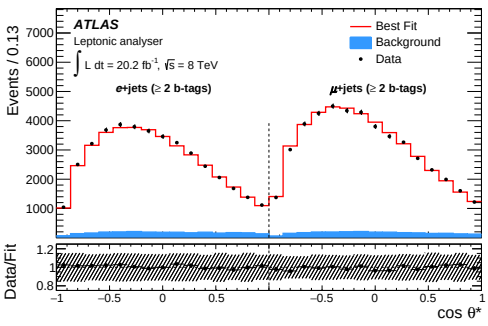

Figure 1: Post-fit distributions of cosθ [12] for the leptonic analyser with ≥ 2 b-tagged jets for e+jets and μ+ jets channels. The band represents the total uncertainty in the fit result.

called polarisation analyzers. The differential distribution of $\cos\theta^*$ allows to distinguish the three contributions associated to the longitudinal, left-handed and right-handed W boson polarisation and it results into an asymmetric $\cos\theta^*$ distribution as the right-handed contribution is negligible.

The value of $\cos\theta^*$ is derived by reconstructing the kinematic properties of the $t\bar{t}$ system through a likelihood fit in selected highly $t\bar{t}$-pure, lepton + jets events. A linear combination of $\cos\theta^*$ templates associated to the different polarisation values are then fit to the data in four regions (e + jets and μ + jets, both with 1 or ≥ 2 b-tagged jets) exemplified in Fig. 1.

The W boson helicity fractions in $t\bar{t}$ decay are obtained with relative uncertainties ranging from 2% to 5% (see Table 1), dominated by systematic effects from b-tagging, jet energy scale and resolution (depending on the polarisation analyzer). The results are consistent with the SM predictions at NNLO accuracy. Anomalous couplings are compatible with zero and they are confined to 95% CL intervals ranging from -0.24 to 0.06.

F_0 = 0.709 $\pm$ 0.012 (stat.+bkg. norm) $^{+0.015}_{-0.014}$ (syst.)
F_L = 0.299 $\pm$ 0.008 (stat.+bkg. norm) $^{+0.013}_{-0.012}$ (syst.)
F_R = -0.008 $\pm$ 0.006 (stat.+bkg. norm) $\pm$ 0.012 (syst.)

Table 1: Measured W boson helicity fractions [12] obtained from the leptonic analyzer. Statistical uncertainty from the fit, from background normalisation and total systematic uncertainty are reported.

3 The Wtb vertex in $t\bar{t}$ production and decay: full spin density matrix

The full spin density matrix for $t\bar{t}$ production and decay is obtained in $t\bar{t}$-enriched dilepton final states [13] by measuring the six angles that the two leptons directions make with respect to a triplet of spin quantisation axis in their respective top-(antitop-)quark parent rest frame. The three axes are: k, the top-quark direction in the $t\bar{t}$ rest frame; n, the axis orthogonal to the plane formed by the k-axis and the direction of the proton beam in the laboratory; r, the versor that is orthogonal to the first two axes.

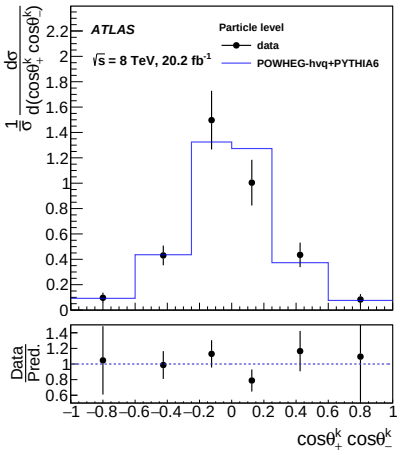

Figure 2: Comparison of the spin correlation distribution and the SM prediction from the signal MC simulation [13]. The total uncertainty is shown in each bin.

The cosines of the six angles $\theta^a_\pm$ are derived from the reconstruction of the kinematic properties of the $t\bar{t}$ system by maximizing the reconstruction probability of the missing transverse momentum in the event ($E_{\mathrm{T}}^{\mathrm{miss}}$). The superscript a refers to the quantisation axis and the subscript +(-) refers to the top (antitop) quark. The distributions of the individual $\cos\theta^a_\pm$ and their products are unfolded to parton level in orde to correct for background and detector effects and to extrapolate to a phase space comparable with theoretical predictions. The averages of such distributions are used to derive fifteen polarisation and spin corrrelation coefficients [8], probing all the elements of the spin density matrix.

The agreement of the unfolded distributions with the SM predictions (an example is shown in Fig. 2 for $cos\theta^k_+ cos\theta^k_-$) indicates that all measured polarisation and spin corrrelation coefficients are consistent with the SM predictions. Systematic uncertainties are just slightly larger than statistical uncertainties and are dominated by $t\bar{t}$ modelling effects. The top-quark polarisation coefficients,

B_s^x, are all zero within the absolute uncertainties of 0.03 to 0.04. The spin correlation coefficients $C(x,x)$, measured with a relative uncertainty of 20%-30% , exclude the "no kk spin correlation" scenario. All the cross-correlation coefficients $C(x,y) \pm C(y,x)$ are found to be consistent with the SM prediction within their absolute uncertainties ranging from 0.08 to 0.17.

4 Charge asymmetry in $t\bar{t}$ production

Another effect influencing the angular distributions of the $t\bar{t}$ pair and their decay products is the NLO interference of $q\bar{q}/qg$ diagrams in the $pp \to t\bar{t}$ strong production. This interference tends to preserve the direction of the colour flow more than it tends to invert it and consequently this leads to the top (antitop) quark being emitted most often in the direction of the incoming quark (antiquark). As the momentum of the valence quark is generally larger than the sea antiquark, the top-quark direction is more forward and backward (less "central") than the antitop quark in the laboratory frame. The difference in the absolute value of rapidity (y) betwen the top and antitop quarks is then used to build the asymmetry $A_C^{t\bar{t}}$ in both the lepton+jets and the dilepton channel defined as

$$A_C^{t\bar{t}} = \frac{N(\Delta|y| > 0) - N(\Delta|y| < 0)}{N(\Delta|y| > 0) + N(\Delta|y| < 0)} \tag{4.1}$$

where $\Delta|y| = |y_t| - |y_{\bar{t}}|$. In the dilepton channel only, the additional diluted asymmetry $A_C^{\ell\ell}$ is derived from the pseudo-rapidities (η) of the charged leptons and defined as

$$A_C^{\ell\ell} = \frac{N(\Delta|\eta| > 0) - N(\Delta|\eta| < 0)}{N(\Delta|\eta| > 0) + N(\Delta|\eta| < 0)} \tag{4.2}$$

where $\Delta|\eta| = |\eta_{\ell^+}| - |\eta_{\ell^-}|$.

The values of y_t and η_{lep} are derived in lepton+jets [14] events by reconstructing the $t\bar{t}$ kinematics through a likelihood fit and in dilepton [15] events by imposing the top-quark mass and W mass constraints and then keeping the solution with (a) the minimum mass of the $t\bar{t}$ system and (b) the lepton-to-b-jet pairing resulting in the largest expected probability to be reconstructed.

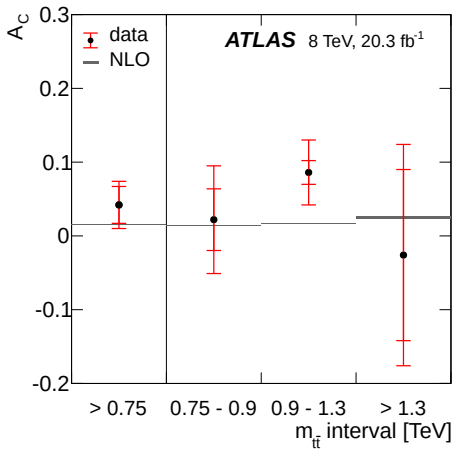

Figure 3: A_c^{tt} values as a function of $m_{t\bar{t}}$ [16]. The error bars on the measurement indicate the modelling and unfolding systematic uncertainties, shown as the inner bar, and the total uncertainty. The SM prediction is shown a shaded horizontal bar in each $m_{t\bar{t}}$bin, where the width of the bar indicates the uncertainty.

The rapidities are also measured as a function of additional variables characterizing the $t\bar{t}$ system like the mass ($m_{t\bar{t}}$), the transverse momentum ($p_{\mathrm{T},t\bar{t}}$) and the absolute value of the boost of the $t\bar{t}$ system along the beam axis ($\beta_{\mathrm{Z},t\bar{t}}$). This enhances the contribution of $q\bar{q}$ annihilation diagrams, particularly in lepton+jets highly boosted events [16] where the products of the hadronic top-quark decay are reconstructed in a large-radius jet in which they are collimated by the large Lorentz boost of the top quark.

The difference of absolute rapidities $\Delta|y|$ and $\Delta|\eta|$ are unfolded to particle and parton level and the $A_C^{t\bar{t}}$ and $A_C^{\ell\ell}$ asymmetries are derived, also in bins of $m_{t\bar{t}}$, $p_{\mathrm{T},t\bar{t}}$ and $\beta_{\mathrm{Z},t\bar{t}}$. The inclusive values of A_c^{tt} and $A_C^{\ell\ell}$ are measured with a relative uncertainty of $\approx 0.5\%$ and summarized in Table 2 with the associated SM predictions. The differential measurements are consistent with zero and with the SM predictions in all the bins of all the measured $t\bar{t}$ variables with absolute uncertainties ranging from 0.03 to 0.24 (for instance A_C^{tt} is shown as a function of $m_{t\bar{t}}$ in Fig.3).

The two asymmetries derived in the dilepton channel are used to test the presence of both heavy and light colour-octect s-channel resonances [15], expected to be unobservable as an excess in the $m_{t\bar{t}}$ spectrum. None of the model predictions, corresponding to a variety of coupling constants to top quarks, is excluded by the measured asymmetries.

On the other hand the phase space for a collection of other models ranging from heavy axigluons to scalar coloured resonances is reduced by $A_C^{t\bar{t}}$ in conjuction with Tevatron A_{FB} using the lepton+jets results [14]. In particular the realisations of a t-channel W' boson are disfavoured over a large fraction of the possible phase space by the lepton+jets boosted results [16].

	dilepton (particle)	dilepton (parton)	lepton+jets (parton)	SM (parton)
A_C^{tt}	0.017 ± 0.018	0.021 ± 0.016	0.009 ± 0.005	0.0111 ± 0.0004
$A_C^{\ell\ell}$	0.006 ± 0.00	$5\ 0.008 \pm 0.006$	-	0.0064 ± 0.0003

Table 2: Inclusive charge asymmetries measured in the lepton+jets [14] and dilepton [15]. The corresponding standard model predictions at parton level [17] are also presented.

5 Charge and CP asymmetry in b-hadrons from $t\bar{t}$ events

Another asymmetry is expected from various sources of CP violation as the probability for a b-quark to decay to a positive muon is different from the probability for the anti-b-quark to decay to a negative muon i.e. in b-quark mixing $P(b \to \bar{b} \to \mu^{\pm}X) \neq P(\bar{b} \to b \to \mu^{\mp}X)$ and in b-quark decay $P(b \to \mu^{\pm}X) \neq P(\bar{b} \to \mu^{\mp}X)$ where $P(Y)$ is the probability for the event Y to occur.

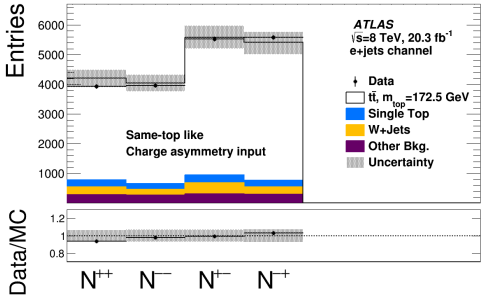

Figure 4: Same-top-like charge-pairings distributions in the e+jets channel from [18] . The hashed area features all experimental systematic uncertainties, the b-hadron production and hadron-to-muon branching ratio uncertainties. The ratio of the data to the simulated prediction is also shown.

This asymmetry is tested in b-quark decays from $t\bar{t}$ lepton + jets events [18]. In these events the charge of the muon from the b-quark decay is measured directly, while the charge of the b-quark is inferred from the charge of the lepton in the $W \to \ell$ decay. The numbers $N^{x,y}$ of events with a given charge for the b-quark (x) and for the μ resulting from its decay (y) are then used to derive the decay probabilities as

$$P(b \to \ell^{+(-)}) = \frac{N^{++(-)}}{N^{++}+N^{+-}};\ P(\bar{b} \to \ell^{+(-)}) = \frac{N^{--(+)}}{N^{--}+N^{-+}} \tag{5.1}$$

and the resulting asymmetries as

$$A^{\mathrm{OS(SS)}} = \frac{P(b \to \ell^{+(-)}) - P(\bar{b} \to \ell^{-(+)})}{P(b \to \ell^{+(-)} + P(\bar{b} \to \ell^{-(+)})} \tag{5.2}$$

where A^{SS} (A^{OS}) is the same- (opposite-sign) charge asymmetry. The asymmetry is decomposed in a linear combination of direct and mixing CP-violation asymmetry contributions as $A^{\mathrm{OS(SS)}} = \sum_i r_i A^i_{\mathrm{mix,dir}}$ where the r_i coefficients are the relative rates of the associated b- and $c-$quark decay channels.

The $N^{x,y}$ distribution of the selected events is obtained by requiring the b-tagged jet to decay to a muon with small transverse momentum (p_T) and by assigning jets and leptons to the $t\bar{t}$ decay products using a likelihood-based kinematic fit. Pairs of bin content in the $N^{x,y}$ distribution, shown in Fig. 4 for e+jets events, are used to build the asymmetries after unfolding the $N^{x,y}$ distribution to particle level.

The measured charge asymmetries and the corresponding CP are illustrated in Table 3. The theoretical CP contributionsare determined in an unconstrained system (two measurements as linear combinations of four asymmetries) by settting all the contributing asymmetries to zero but one, in

	Data (10^{-2})	MC (10^{-2})	SM prediction (10^{-2})
A^{SS}	-0.7 ± 0.8	0.05 ± 0.23	$<10^{-2}$
A^{OS}	-0.4 ± 0.5	-0.03 ± 0.13	$<10^{-2}$
A^{b}_{mix}	-2.5 ± 2.8	0.2±0.7	$<10^{-3}$
$A^{b\ell}_{dir}$	0.5±0.5	-0.03±0.14	$<10^{-5}$
$A^{c\ell}_{dir}$	1.0±1.0	-0.06±0.25	$<10^{-5}$
A^{bc}_{dir}	-1.0±1.1	0.07±0.29	$<10^{-7}$

Table 3: Comparison of measurements of charge asymmetries and constraints on CP asymmetries, with MC simulation (detailed in the text), existing experimental limits and SM predictions from [18]

turn. All the results are consistent with zero, with the SM NLO Monte Carlo predictions and with the upper limits derived from fixed order calculations.

6 Measurememt of the top-quark width

The top-quark width Γ_t is measured at ATLAS for the first time in lepton +jets events [19] by using two variables that are reconstructed by assigning jets and leptons to the $t\bar{t}$ system by a kinematic likelihood fit. The first variable is $m_{\ell b}$, the invariant mass of the lepton and b-jet, both assigned to the leptonic top-quark decay: its shape is sensitive to Γ_t and it is less sentive to jet energy scale systematic effects than other hadronic masses as only one jet is used for its reconstruction. The second variable is the $\Delta R_{min}(j_b, j_i)$ [1] between the b-jet and the closest light jet to the b-jet itself, both assigned to the hadronic top-quark decay. Although this variable has almost no shape sensitivity to the top-quark width, it turns out to help reduce the jet energy scale systematic uncertainty when templates of $m_{\ell b}$ and $\Delta R_{min}(j_b, j_i)$ with varying Γ_{top} are used for a simultaneous maximum likelihood fit to the data in eight signal regions. Fig. 5 shows fit results for the two variables in two different signal regions. The top-quark width is extracted and its value is $\Gamma_t = 1.76 \pm 0.33\,(\text{stat})\,^{+0.79}_{-0.68}\,(\text{syst})$ GeV for a top-quark mass of 172.5 GeV. The total uncertainty of 49% is dominated by systematic effects due to jet energy scale ($\approx 24\%$) and $t\bar{t}$ generator modelling uncertainty. The result is consistent with the SM prediction.

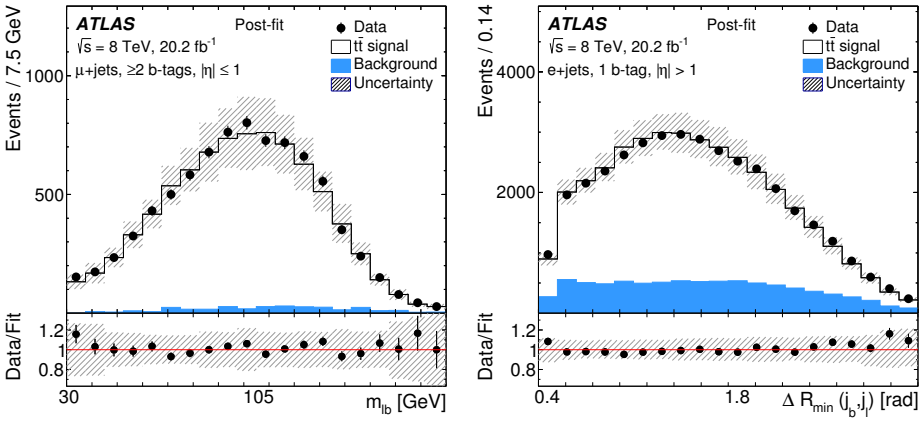

(a) (b)

Figure 5: Examples for post-fit distributions for (a) $m_{\ell b}$ and (b) $\Delta R_{min}(j_b, j_i)$ from [19]. The lower panel shows the ratio of data to post-fit sum of $t\bar{t}$ signal and background. The band shows the total uncertainty.

[1] ΔR is the angular distance between two four momenta defined as $\sqrt{(\Delta\eta)^2 + (\Delta\phi)^2}$ where $\Delta\eta$ ($\Delta\phi$) are the differences in pesudo-rapidity (azimuthal angle) between the spatial directions associated the two four momenta.

7 Conclusions

Given the mass and the SM gauge couplings of the top quark, its spin properties are imprinted in the angular distributions of its decay products. Additional correlations are caused by angular asymmetries arising from NLO interference in $t\bar{t}$ production and by CP violation in b-quark decays from $t\bar{t}$ pairs.

ATLAS measurements of angular and asymmetry properties in top-quark production and decay using data collected in LHC pp collisions at $\sqrt{s}$ = 8 TeV agree with SM predictions. ATLAS measurements probed the Wtb vertex and its convolution with $t\bar{t}$ strong production.The degree of W polarisation is known at 2-5% (relative), the degree of top polarisation is determined at 1-4% level (absolute) and the degree of $t\bar{t}$ spin correlations is tested at O(10-20)% (relative). The $q\bar{q}$ NLO interference effects in $t\bar{t}$ production are tested at 10^{-2} precision inclusively and at the 3-15% precision differentially while the SM predicts effects of order 10^{-2} to 10^{-3}. CP violation in b-quark decay from $t\bar{t}$ events is tested at the 10^{-2} level and the SM predicts a $< 10^{-2}$ effect.

The first ATLAS top-quark width direct measurement used data collected in LHC pp collisions at $\sqrt{s}$ = 8 TeV. It achieves 49% relative uncertainty and it is consistent with the SM.

As no evidence for effects of physics beyond the SM is observed, the ATLAS collaboration looks forward to analyzing the new incoming data at $\sqrt{s}$= 13 TeV the LHC is currently delivering.

References

[1] C. Patrignani et al. (Particle Data Group), Chin. Phys. C, 40, 100001 (2016) and 2017 update.

[2] T. Stelzer and S. Willenbrock, Phys. Lett. B **374**, 169 (1996) [hep-ph/9512292].

[3] A. F. Falk and M. E. Peskin, Phys. Rev. D **49**, 3320 (1994) [hep-ph/9308241].

[4] G. Mahlon and S. J. Parke, Phys. Rev. D **81**, 074024 (2010) [arXiv:1001.3422 [hep-ph]].

[5] S. J. Parke, Nuovo Cim. C **035N3**, 111 (2012) [arXiv:1202.2345 [hep-ph]].

[6] J. H. Kuhn and G. Rodrigo, Phys. Rev. D **59**, 054017 (1999) [hep-ph/9807420].

[7] O. Gedalia, G. Isidori, F. Maltoni, G. Perez, M. Selvaggi and Y. Soreq, Phys. Rev. Lett. **110**, no. 23, 232002 (2013) [arXiv:1212.4611 [hep-ph]].

[8] W. Bernreuther, D. Heisler and Z. G. Si, JHEP **1512**, 026 (2015) [arXiv:1508.05271 [hep-ph]].

[9] ATLAS Collaboration, 2008 JINST 3 S08003

[10] See R. Nisius, these proceedings

[11] See M. Alhroob,these proceedings, K. Kawade, these proceedings, C. Pollard, these proceedings

[12] ATLAS Collaboration, Eur. Phys. J. C **77**, no. 4, 264 (2017) [arXiv:1612.02577 [hep-ex]].

[13] ATLAS Collaboration, JHEP **1703**, 113 (2017) [arXiv:1612.07004 [hep-ex]].

[14] ATLAS Collaboration, Eur. Phys. J. C **76**, no. 2, 87 (2016) [arXiv:1509.02358 [hep-ex]].

[15] ATLAS Collaboration, Phys. Rev. D **94**, no. 3, 032006 (2016) [arXiv:1604.05538 [hep-ex]].

[16] ATLAS Collaboration Phys. Lett. B **756**, 52 (2016) [arXiv:1512.06092 [hep-ex]].

[17] W. Bernreuther and Z. G. Si, Phys. Rev. D **86**, 034026 (2012) [arXiv:1205.6580 [hep-ph]].

[18] ATLAS Collaboration, JHEP **1702**, 071 (2017) [arXiv:1610.07869 [hep-ex]].

[19] ATLAS Collaboration, arXiv:1709.04207 [hep-ex].